Eur. Phys. J. A **31**, 1–7 (2007)
DOI 10.1140/epja/i2006-10158-9

THE EUROPEAN PHYSICAL JOURNAL A

Regular Article – Nuclear Structure and Reactions

Decay study of neutron-rich zirconium isotopes employing a Penning trap as a spectroscopy tool

S. Rinta-Antila[a], T. Eronen, V.-V. Elomaa, U. Hager, J. Hakala, A. Jokinen, P. Karvonen, H. Penttilä, J. Rissanen, T. Sonoda, A. Saastamoinen, and J. Äystö

University of Jyväskylä, Department of Physics, P.O. Box 35 (YFL), FIN-40014 Jyväskylä, Finland

Received: 29 September 2006
Published online: 18 January 2007 –
Communicated by D. Guerreau

Abstract. A new technique to produce isobarically pure ion beams for decay spectroscopy by using a gas-filled Penning trap was commissioned at the ion guide isotope separator on-line facility, IGISOL. β-decays of neutron-rich ^{100}Zr, ^{102}Zr and ^{104}Zr isotopes were studied with this technique. In addition, the Q_{β^-} values of ^{100,102,104}Zr β-decays were determined from the direct mass measurements of zirconium and niobium isotopes performed with a high-precision Penning trap. The mass of ^{104}Nb was directly measured for the first time and the obtained mass excess value for the longer-living (1^+) state is -71823 ± 10 keV. For the ground states of ^{100}Nb and ^{102}Nb the obtained mass excess values were -79802 ± 20 keV and -76309 ± 10 keV, respectively. The observed distribution of the β strength supports a prolate deformation assignment for ^{100,102,104}Zr isotopes.

PACS. 07.75.+h Mass spectrometers – 21.10.Dr Nuclear structure: Binding energies and masses – 27.60.+j $90 \leq A \leq 149$ – 23.40.-s β decay; double β decay; electron and muon capture

1 Introduction

Neutron-rich zirconium isotopes have some extraordinary features, such as the sudden change of nuclear shape when increasing the neutron number from 56 to 60. This region of rapid shape change has been experimentally studied by methods which employed the β-decay of parent yttrium nuclei [1], prompt fission fragment γ-ray measurements [2], collinear laser spectroscopy [3] and most recently direct mass measurements [4,5]. The problem of allowed unhindered β-decays of deformed nuclei was recently studied theoretically by Urkedal *et al.* [6]. They showed that in the neutron-rich region of $Z \approx 40$ the Gamow-Teller strength B(GT) distribution at very low excitation energy depends on the magnitude and the sign of the deformation and can therefore provide further insight into the evolution of deformation in these nuclei. Since neutron-rich ^{100}Zr, ^{102}Zr and ^{104}Zr are among the most strongly deformed nuclei their β-decay properties are of great interest to study.

Decay spectroscopy of rare isotopes becomes difficult at conventional isotope separator on-line (ISOL) facilities when going far from stability due to high background generated by the nuclei within the same isobaric chain. Generally, in-flight fragment separators do not suffer from this limitation but the radioactive products are implanted deep in the focal-plane detector which may limit the resolution and sensitivity. To increase the selectivity of the ISOL technique, element selective ionisation can be used, for example by resonant laser ionisation. Another option is to use high-resolving-power mass separation. A variant of the latter approach is adopted in this work as we have used a gas-filled Penning trap to mass separate a beam of a single isotope from the IGISOL beam. The method was used to produce purified beams of neutron-rich zirconium isotopes for a subsequent decay study.

In the experiment reported here, the focus was on improving quantitatively the knowledge of the β-decay properties of zirconium nuclei. In particular, their ground-state branching ratios and Q_{β^-} values are needed in order to extract the Gamow-Teller strength distributions.

Table 1. The properties of isomeric states in ^{100,102,104}Nb tabulated in NUBASE03 [7].

Nuclide	E_{exc} [keV]	$t_{1/2}$ [s]	J^π
^{100}Nb	0	1.5(2)	1^+
^{100m}Nb	470(40)	2.99(11)	$(4^+,5^+)$
^{102}Nb	0	1.3(2)	1^+
^{102m}Nb	130(50)	4.3(4)	high
^{104}Nb	0	4.9(3)	(1^+)
^{104m}Nb	220(120)	0.940(40)	high

[a] e-mail: sami.rinta-antila@phys.jyu.fi

The daughter niobium nuclei are known to have two β-decaying states. The tabulated properties of niobium nuclei are listed in table 1.

2 Experimental method

The measurements were carried out at the ion guide isotope separator on-line (IGISOL) facility at the University of Jyväskylä [8,9] in two separate experiments. Neutron-rich zirconium isotopes were produced by 30 MeV proton-induced fission of a natural uranium target. After stopping the fission fragments in the ion guide buffer gas as 1^+ ions, they were accelerated to 30 keV energy and mass separated with a 55 degree dipole magnet. The separated beam was injected into a gas-filled radio frequency quadrupole cooler and buncher (RFQ) [10]. Acting as the first stage of the JYFLTRAP system, the RFQ transforms the low-quality dc-beam from IGISOL to a low emittance and bunched ion beam required for the injection into the Penning trap.

The purification trap of the JYFLTRAP system [11] uses a buffer gas cooling technique for mass selection. The isobaric purification is achieved by first exciting all ions in the trap to a larger radius using a dipole excitation with a mass-independent magnetron frequency. After this excitation the ions are mass selectively centered onto the trap axis by applying a quadrupole excitation with the true cyclotron frequency $\nu_c = 1/2\pi \cdot q/m \cdot B$. This converts the slow magnetron motion to a fast reduced cyclotron motion. The ions lose their energy quickly in collisions with 10^{-4} mbar helium buffer gas atoms. As a result the radius of the radial motion vanishes and the selected ions are centered. Finally, extraction through a narrow channel of 1 mm in radius cleans all the unwanted ions from the ion bunch. The mass resolving power $M/\Delta M$ that was reached with a 220 ms purification cycle was of the order of 50000, that is clearly sufficient to separate studied isotopes of zirconium from their neighbouring isobars, see fig. 1.

The purified ion sample can be either sent through the second precision trap to the spectroscopy set-up or captured in the precision trap for a mass measurement [12]. To determine the β-decay energy Q_β for each studied decay the atomic masses of the mother and daughter isotopes were measured with the precision trap using time-of-flight (TOF) technique [13], see also ref. [5].

In a normal measurement cycle, the ions are kept in each step (RFQ, purification trap and precision trap) only the minimum time required to perform the necessary manipulations. This kind of cycle is hereafter referred to as a *direct* measurement cycle. Other cycle timing used in the mass determination of the niobium isotopes, which have two β-decaying isomeric states with different half-lives, is called *delayed* measurement cycle. In the delayed cycle the ion bunch was kept in the purification trap for 4 seconds before applying dipole and quadrupole excitations. During the delay the abundances of isotopes in the trap evolve according to the half-lives.

The isobarically purified samples of the desired isotopes were implanted with 30 keV energy into a movable tape surrounded by the detector set-up. Data collection and source implantation into a fresh part of the tape were always started simultaneously and continued typically for 1–3 h depending on the production yield. In the first experiment the detector set-up consisted of a thin, planar plastic scintillator to detect β-particles, and a large germanium detector for γ-ray detection on the opposite side of the implantation point. The event data was collected in singles mode (both detectors triggering the acquisition), enabling determination of the β efficiency from the on-line data. For the second experiment, the detector set-up was improved by adding another large germanium detector and a planar low-energy germanium detector (LEGe) to detect low-energy γ-rays and X-rays. Also, the planar plastic scintillator was replaced by a cylindrical scintillator surrounding the implantation point leading to a 7-fold efficiency increase compared to the earlier set-up. Most of the time the acquisition was triggered by β- or LEGe-singles or γ-γ coincidences.

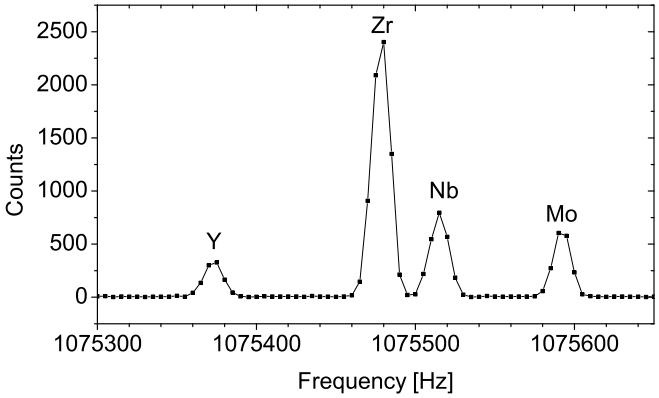

Fig. 1. A quadrupole frequency scan in the purification trap for mass $A = 100$. Each point is accumulated for 50 cycles and the full spectrum was collected in 30 min.

3 Results

Because the Penning trap is used as a high-resolving-power mass separator, the produced source contains only one isotope and any daughter activity present in the sample grows in only via the decays of implanted mother nuclei. The amount of β-decays coming from zirconium can be calculated from the total number of observed β-particles by using the decay law and known half-lives of the members of the decay chain. On the other hand, β feedings to excited states can be deduced from the γ intensities. The ground-state branching is simply the difference between these two divided by the total number of zirconium β-decays. An example of β-gated γ spectra obtained with ^{100,102,104}Zr gates in the purification trap are shown in fig. 2. A comparison between two γ spectra recorded after applying isobaric purification for ^{102}Nb and ^{102}Zr, respectively, can be found in ref. [14].

Only in the case of ^{100}Nb was the decay scheme of the low-spin ($J^\pi = 1^+$) state known well enough to deduce

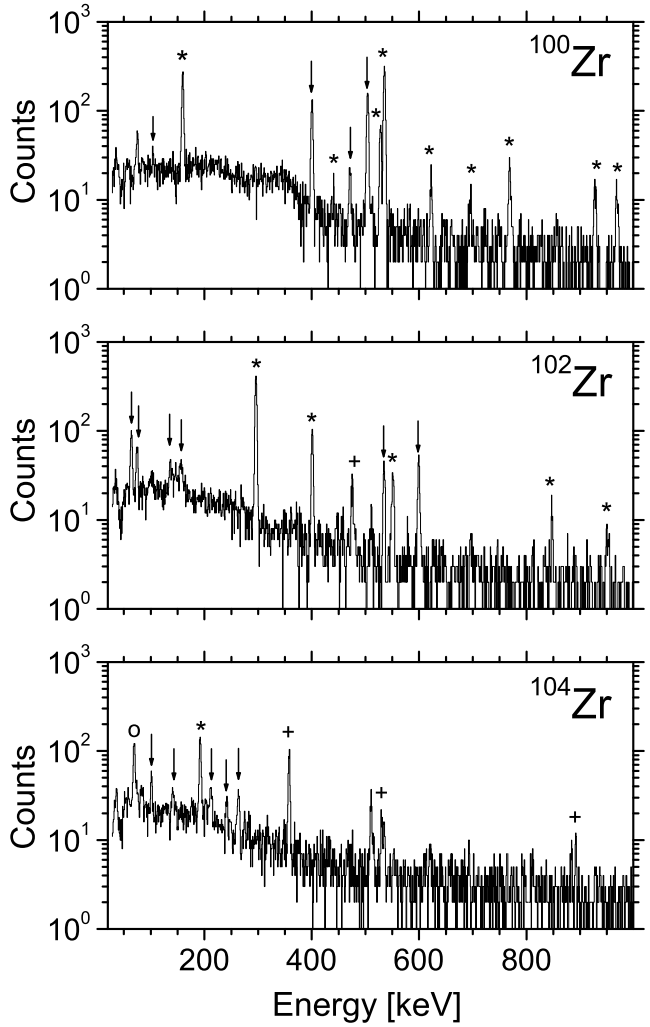

Fig. 2. β-gated γ spectra obtained with ^{100,102,104}Zr gates. The strongest peaks from the decay of zirconium are indicated with arrows. Transitions in molybdenum are marked with an asterisk (*), in ruthenium with plus sign (+), and in technetium with open circle (○).

the number of parent ^{100}Zr decays. Using the intensity of the strong 535 keV $2^+ \rightarrow 0^+$ transition in ^{100}Mo gives a slightly higher value for the number of zirconium decays compared to the one deduced from the gross β counting, however they agree within the uncertainties. Since the transition intensities following the decays of the 1^+ states in ^{102}Nb and ^{104}Nb are not known, similar cross-checking is not possible in these isobars.

The experimental results and their comparison to the earlier reported decay schemes are discussed in the following three sections for each studied zirconium isotope. In sect. 3.4 the Q_β determination is discussed.

Particularly for ^{102}Zr and ^{104}Zr the given intensities are upper, and $\log ft$ values lower limits only, as there is probably some feeding to the higher-lying levels which is missed due to limited detection sensitivity. The fraction of the missed intensity is potentially increasing with the Q_{β^-} value.

3.1 Decay of ^{100}Zr

Our γ-decay data agrees with the existing data in the literature [15]. The two strongest transitions observed are at 504 keV and 401 keV. Uncertain 197 keV and 695 keV transitions in the previous work were not seen or could not be assigned to this decay as there is a 695 keV transition in the decay of the daughter nucleus ^{100}Nb. In addition to previously known transitions, we could assign two new transitions (471 keV and 33 keV) to the decay of ^{100}Zr as identified from their X-ray coincidences. In the γ spectrum gated with the niobium K_α X-ray at 16.6 keV we find strong 401 keV and 471 keV transitions. Gating with the 471 keV transition results in a clear 33 keV peak together with the 16.6 keV X-ray peak pointing to a high conversion coefficient for the 33 keV transition. From the fluorescent production a conversion coefficient $\alpha_K = 3.1(8)$ can be deduced. In the compilation of Band *et al.* [16], α_K for a 33 keV $M1$ is 4.78(8), for $E1$ 2.46(4), and for $E2$ 31.7(5). The coincidence spectrum of the 33 keV transition has only one strong peak at 471 keV. The order of the 33 keV and 471 keV transitions is based on the intensities assuming a total conversion coefficient of $\alpha = 3.5$ for the 33 keV transition. The transition energies of 33 keV and 471 keV sum up to 504 keV which agrees with the 504 keV 1^+ level energy.

The ground-state β feeding was determined to be 45(4)%. Other strongly fed states are at 504 keV and 401 keV with $\log ft$ values of 4.49(6) and 4.79(7), respectively. Based on their strong β feeding, a 1^+ assignment is adopted for these levels.

Because the 103.7 keV transition is between two 1^+ states it is most likely of the $M1$ type. Its theoretical [16] internal conversion coefficient $\alpha = 0.2039(29)$ leads to a total intensity $I_{\gamma+ce} = 1.10(10)$. Because the other transitions have higher energy, the conversion has no effect and it has been omitted in the intensity assignment. The decay scheme showing the total transition intensities and $\log ft$ values is shown in fig. 3.

3.2 Decay of ^{102}Zr

The observed γ-transition intensities and energies were used together with the earlier reported data [17] to produce a decay scheme of ^{102}Zr, which is shown in fig. 4. The strongest transitions in this decay have energies of 64 keV, 535 keV, and 599 keV. They form a similar pattern as in the isotone ^{100}Y and are proposed to be related to the $K^\pi = 1^+$ bands [18].

Earlier data compiled in Nuclear Data Sheets [17] is internally inconsistent as the given transition intensities to the lowest state sum up to 79.27%, leaving 20.73% for the direct β-branch to the state instead of the given 43%.

X-ray fluorescence was used to determine conversion coefficients when possible. For the 20.4 keV transition we deduced $\alpha_K = 7.9 \pm 2.5$ which points to $E1$ ($\alpha_K^{th} = 9.0 \pm 0.3$) or at most $M1$ ($\alpha_K^{th} = 20.0 \pm 0.6$). The other multipolarities give $\alpha_K > 60$. Similarly for the 64.5 keV

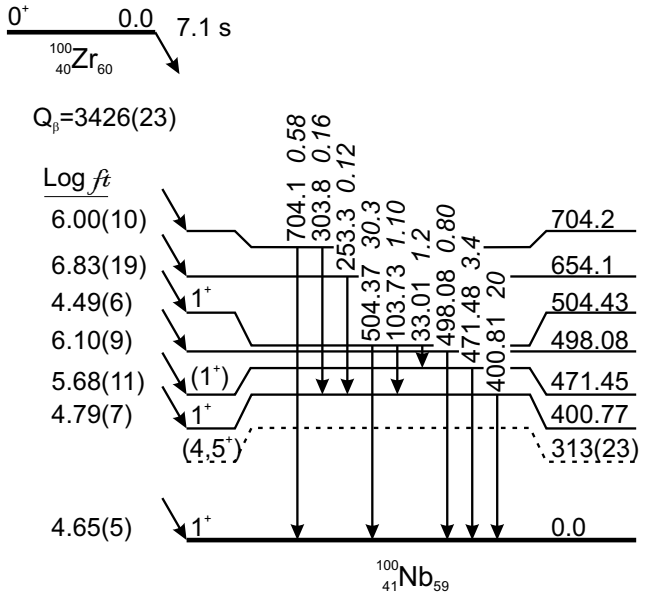

Fig. 3. The decay scheme of ^{100}Zr. The intensities given are $I_{\gamma+ce}$ per 100 β-decays. The 313 keV level drawn with a dashed line is the excited isomeric state, its new energy assignment is based on our mass measurement. The ground-state feeding upper limit is deduced as 45(4)%.

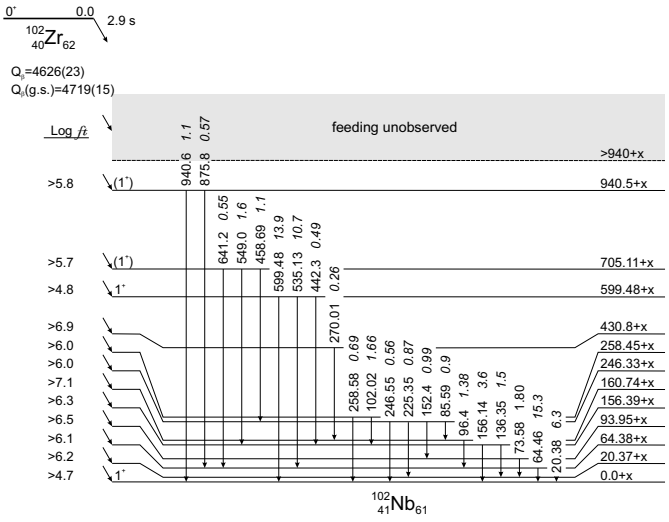

Fig. 4. The decay scheme of ^{102}Zr. The given intensities are $I_{\gamma+ce}$ per 100 β-decays. Based on our mass measurement the energy offset x is 93 ± 23 keV. The ground-state feeding upper limit is deduced as 59(3)%.

transition we obtained $\alpha_K = 0.78 \pm 0.16$ which is in agreement with the $M1$ assignment ($\alpha_K^{th} = 0.686 \pm 0.021$). The $M1$ nature of the transition also agrees with a tentative spin and parity assignment of 2^+ for the $x + 64$ keV state in [18]. In ref. [17] all low-energy transitions are assumed to be of $M1$ nature in the calculation of the conversion coefficients. We assume that the 20.4 keV transition has an $E1$ multipolarity and use the theoretical $\alpha_{tot} = 10.3$ to deduce its total intensity. According to this selection, the $x + 20.4$ keV state would have a negative parity and therefore it has only weak direct β feeding.

The Gamow-Teller strength to low-lying states is mostly shared between the $x+599$ keV state and the $x+0$ keV state. The spin and parity assignment of these states is therefore 1^+.

3.3 Decay of ^{104}Zr

The decay scheme of ^{104}Zr as deduced from this work and ref. [19] is shown in fig. 5. The first two excited states fed in the ^{104}Zr decay lie at very low energies, 8.5 keV and 37.4 keV. Internal conversion is dominant, especially in the case of the 8.5 keV transition. In fact, we see no peak with this energy in the γ spectrum. Furthermore, as the K conversion is energetically forbidden, mostly L conversion takes place. However, due to the detection threshold, L X-rays at 2.2 keV could not be seen. Evidence for this transition arises from the energy differences of transitions de-exciting higher-lying levels. The total intensity of this transition is deduced with the assumption that there is no direct β feeding to this state. An $E1$ nature was adopted for the conversion coefficient calculation.

The second excited state at 37.4 keV de-excites via converted 28.8 keV and 37.4 keV transitions. The fluorescence yield could not be used in this case as there are two converted transitions from the same state. Assuming the 37.4 keV transition to be $M1$ and the 28.8 keV transition to be $E1$, and no β feeding to the lowest excited state leads to a ground-state feeding of 76(6)% and $\log ft = 4.8$. In turn this leads to a tentative spin and parity assignment of 1^+ for the ground state. The same assumptions give a $\log ft$ of 5.7 for the 37.4 keV state and a tentative $J^\pi = 1^+$ assignment.

The 514 keV state is also quite strongly fed with $\log ft = 5.6$. In the previous literature the 250 keV and 311 keV states have been tentatively assigned as 1^+. This

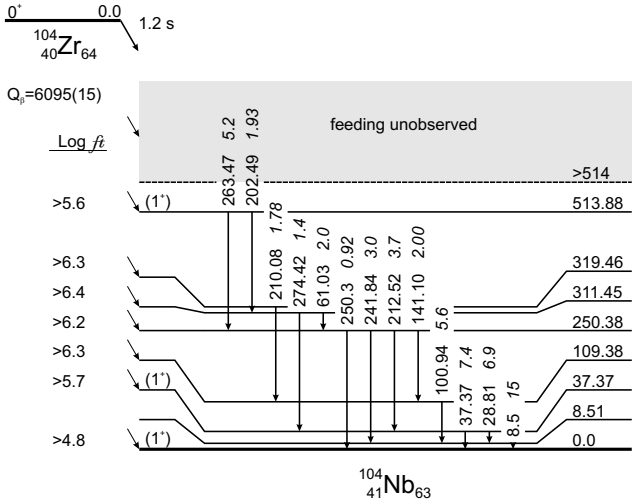

Fig. 5. The decay scheme of ^{104}Zr. The given intensities are $I_{\gamma+ce}$ per 100 β-decays. The ground-state feeding upper limit is deduced as 76(6)%.

assignment is based on JOSEF on-line separator data given in ref. [18], and the observation of a similar band in the isotone ^{102}Y. Based on our new data, these states are not as strongly fed but rather have log ft 6.2 and 6.4, respectively. These do not support 1^+ assignments.

3.4 Decay Q values

The earlier experimental data on Q_β values of even neutron-rich zirconium isotopes ends at $A = 102$. They are obtained from β-decay endpoint energy measurements [20,21]. In this work we measured the masses of the daughter niobium isotopes with the JYFLTRAP set-up. With inclusion of the masses of the zirconium isotopes measured in our earlier experiment [5] the Q_β values of zirconium β-decay could be deduced. In these measurements ^{97}Zr or ^{102}Ru were used as the reference masses. An experimental challenge was introduced by the fact that the even-mass niobium isotopes are known to have two β-decaying states. In the recent mass compilation [7] the energy differences of 470 ± 40 keV, 130 ± 50 keV, and 220 ± 120 keV are given for the isomeric states in ^{100}Nb, ^{102}Nb, and ^{104}Nb, respectively. No transitions between these states have been reported. Because it is difficult to measure masses of isotopes having close-lying isomeric states, especially when the production yields of the states differ significantly from each other, we used a delayed measurement cycle to improve the sensitivity and to help in the state identification.

In a direct time-of-flight resonance scan of ^{100}Nb shown in fig. 6a) one strong resonance is seen at ν_C = 1075391.26 Hz. A closer analysis reveals a second component at a higher frequency ν_C = 1075394.89 Hz corresponding to a lower energy and mass. Two resonances were fitted to the data obtained with three different excitation times 400 ms, 800 ms and 1 s. The obtained mass excess of the excited isomeric state is -79488 ± 10 keV. This value agrees with the mass excess value of -79471 ± 28 keV reported for ^{100m}Nb with a 2.99 s half-life in the Atomic Mass Evaluation 2003 (AME03) [22]. Due to its lower intensity the ground-state mass excess could not be determined as accurately but the value of -79802 ± 20 keV was derived leading to 313 ± 23 keV energy difference between the two states. This mass excess and excitation energy differs by 130 keV from the AME03 value.

In a direct measurement the intensity ratio of the ground state to the higher-energy isomeric state is found to be about 15%. This intensity ratio is increased to ∼30% in the delayed measurement, fig. 6b). Since the relative intensity of the ground state is higher in the delayed measurement, it means that either the half-life of the ground state is longer than that of the excited isomeric state or the feeding of the ground state due to in-trap β-decay of ^{100}Zr increases its relative yield. Since ^{100}Zr is produced more in the reaction than ^{100}Nb (as seen from fig. 1), its decay can change the ratio of the two measured states in the observed way. However, the chemistry taking place and the ion survival in the trap after the decay are uncertain. Therefore, in connecting the mass values to the half-life and J^π data we have to rely mainly on an earlier

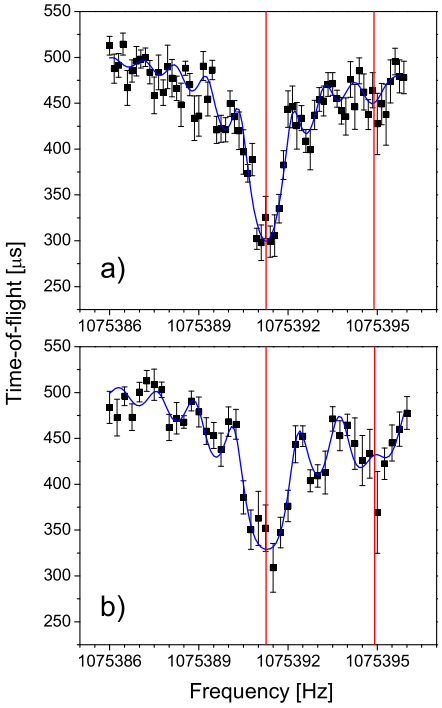

Fig. 6. Resonance time-of-flight spectra of ^{100}Nb. Two fitted resonance positions are marked with vertical lines a) for direct measurement with 1 s excitation and b) for 4 s delayed measurement with 800 ms excitation.

Q_{β^-} value measurement of ^{100}Zr [23]. This leads to the conclusion that the ground state is the 1^+ state and the excited isomeric state is the high-spin state. As mentioned above this assignment is also in agreement with an earlier Q value measurement of the ^{100}Mo(t,^{3}He)^{100}Nb charge exchange reaction [24] if the interpretation of the data by Wapstra *et al.* [25] is adopted. The authors of [24] assumed the peak detected with the highest energy to correspond to the 1^+ final state. However, their large detection angle seems to favour population of higher-spin states. Therefore, the low-spin ground state may have been missed. In fact, to agree with the β endpoint measurements [26] Audi *et al.* have identified the state measured in the reaction study as the high-spin isomeric state.

The direct time-of-flight resonance curve of ^{102}Nb shown in fig. 7a) is asymmetric. This asymmetry could be induced by a close-lying isomeric state. Fitting two resonances to the five individual TOF scans results in a mean difference of 1.04 Hz for their positions. In fig. 7a) the solid line is a result of the fit to two and the dashed line to only one resonance. The solid line corresponds to a better fit (χ^2/DoF decreases from 1.75 to 1.31). When the ion bunch is delayed in the first trap for 4 s before the measurement, the resonance becomes symmetric and the excited isomer seems to vanish, see fig. 7 b). This is contradictory with the literature data [7] that reports half-lives of 1.3 s for the ground state and 4.3 s for the excited isomer. Therefore, the result implies that the ground state is the longer-lived high-spin state. In this isobar ^{102}Zr is so weakly produced, only 1/12 of the ^{102}Nb yield, that its de-

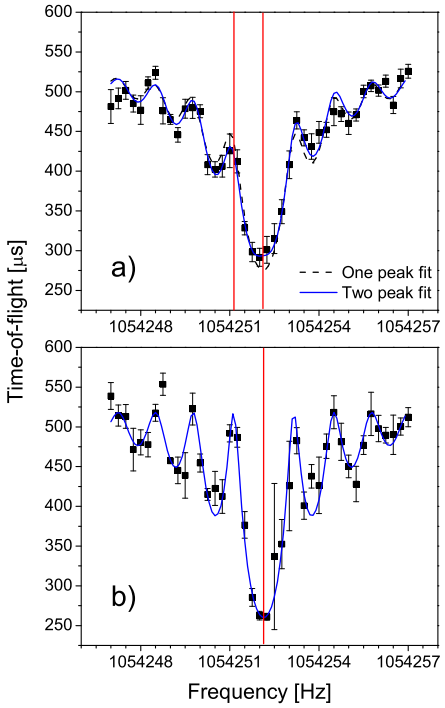

Fig. 7. Time-of-flight resonance curves of ^{102}Nb with 800 ms excitation time. The fitted resonance positions are marked with vertical lines. a) The direct measurement. The dashed line is a fit to a single and the solid line to two resonance curves. b) The 4 s delayed measurement has only a single peak fit.

Table 2. Q_{β^-} values from zirconium ground state to the niobium β-decaying low-spin state. New values are compared to the tabulated ones from ref. [22].

Isotope	Q_β [keV]	AME03 Q_β [keV]
^{100}Zr	3426 ± 23	3335 ± 25
^{102}Zr	4626 ± 23	4610 ± 30
^{104}Zr	6095 ± 15	$5880 \pm 410^*$

* Value and uncertainty derived from systematic trends.

cay to ^{102}Nb in the first trap does not impact significantly the intensity ratio between ^{102}Nb and ^{102m}Nb (unlike in the mass $A = 100$). The mass excess values for the two states are -76309 ± 10 keV and -76216 ± 20 keV for the ground and the excited isomeric 1^+ state, respectively. These values lead to an excitation energy of 93 ± 23 keV for the low-spin isomeric state. Due to small separation between these two states and the reached resolution with the 800 ms excitation time the mass of the isomeric state should be taken as a tentative value.

According to figs. 8 a) and b) only one resonance is seen for ^{104}Nb. After 4 s delay in the first trap the position of the main peak remained the same as compared to the direct TOF resonance. After the 4 s delay time hardly any amount of the 940 ms state is left. Therefore, the longer-living (1^+) state can be quite confidently identified. For this resonance a mass excess of -71823 ± 10 keV can be determined.

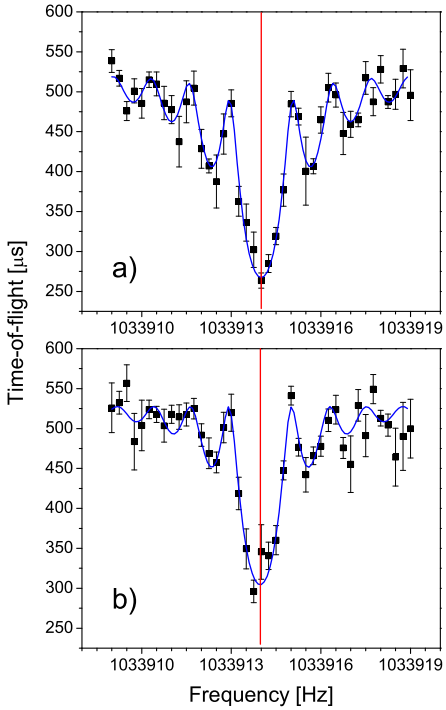

Fig. 8. TOF resonance of ^{104}Nb detected by using 800 ms excitation time from a) direct measurement and b) 4 s delayed measurement.

The Q_{β^-} values shown in table 2 were deduced using the above-mentioned mass excess values for niobium isotopes and the ones reported earlier for the zirconium isotopes [5].

4 Discussion

The β strength distributions of the ^{100,102,104}Zr isotopes have been studied with significantly improved precision. The Q_β value of ^{104}Zr has been determined for the first time. With these measurements it has been shown that the Penning trap can be used as a powerful tool in nuclear spectroscopy in addition to its use for precision atomic-mass measurements.

It is of particular interest to look at the Gamow-Teller (GT) strength distributions of the studied nuclei in light of a recent theoretical calculation by Urkedal and Hamamoto [6] and of our earlier work on nearby neutron-rich Mo isotopes [27,28]. Using a Skyrme-type Hartree-Fock calculation plus the Tamm-Dancoff approximation or random-phase approximation, Urkedal *et al.* have searched for neutron-rich nuclei that would have considerable GT strength ($B(\mathrm{GT}) \sim 1$) at low excitation energies. In the neutron-rich zirconium region the active asymptotic orbitals that contribute to unhindered GT β-decay are $[413\ 5/2]_\mathrm{n}$ and $[413\ 7/2]_\mathrm{p}$ for the neutron and proton, respectively. Strong GT strength at low energy can be expected when both orbitals are close to their Fermi levels.

It is found in ref. [6] that for oblate deformation the low-lying GT strength consists of many weak transitions,

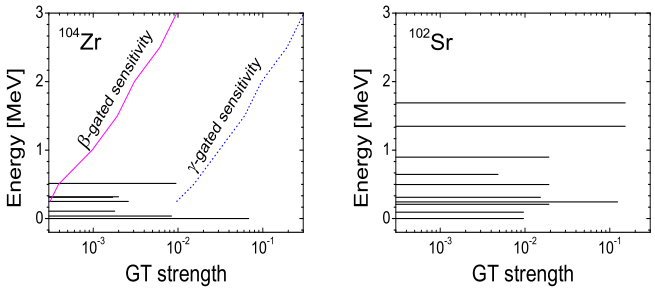

Fig. 9. Observed GT strengths and detection sensitivity limits in the case of ^{104}Zr decay. Detection sensitivity limits are estimated for 2σ peaks. The γ-gated detection limit is calculated assuming coincidence with a 250 keV transition. The second graph shows a similar plot for ^{102}Sr (two protons lighter isotone of ^{104}Zr) as a comparison. The strontium data is from ref. [17].

whereas for prolate deformation a relatively strong GT strength is expected deriving from the spin-orbit partner $\Lambda \pm 1/2$ orbitals for neutrons and protons, respectively. The latter decay leads to a strong population of only a few states as observed for all studied zirconium isotopes suggesting a prolate deformation. A similar behaviour has been observed earlier for the decays of even n-rich molybdenum isotopes [27,28]. In order to confirm this statement an extension of the calculations of ref. [6] would be highly desirable. The equilibrium shapes in the zirconium region nuclei have also been calculated using the Nilsson-Strutinsky method by Skalski *et al.* [29]. Their calculations agree with the prolate assignment as they produce a strongly prolate deformed potential minimum 0.85 to 1.67 MeV lower in energy than the coexisting oblate minimum when going from ^{100}Zr to ^{104}Zr.

Although the GT strength distributions to low-lying energy states are consistent with calculations having a prolate deformation, the observed total GT strength for the studied zirconium isotopes is relatively small. It goes down from $B_\Sigma(\mathrm{GT}) = 0.29$ for ^{100}Zr to only $B_\Sigma(\mathrm{GT}) = 0.094$ for ^{104}Zr. This could be due to missed feeding of higher-lying 1^+ states. Figure 9 shows the observed Gamow-Teller strength distribution for ^{104}Zr decay together with β-gated and γ-gated detection limits for a 2σ γ-ray peak. The β-gated limit is the limit to detect the known transitions whereas the γ-gated limit is a limit for assigning the transition. It is interesting to compare these zirconium decays to decays of strontium, their lighter isotones. ^{100}Sr and ^{102}Sr exhibit a very similar decay pattern as ^{102}Zr and ^{104}Zr at low energy but they have much higher total observed GT strengths $B_\Sigma(\mathrm{GT}) = 0.45$ and $B_\Sigma(\mathrm{GT}) = 0.53$, respectively. This is mainly due to a substantial feeding to states around 1 and 1.5 MeV. If we assume a similar state with $\log ft = 4.4$ at 1.7 MeV as seen in ^{102}Sr decay, branching to this state in the ^{104}Zr decay should be 40%. According to detection limits shown in fig. 9 such a strong branching should be visible. However, a significantly higher production rate of ^{104}Zr is needed to clarify this question which is also of general importance for a better understanding of β-decays of highly neutron-rich nuclei in this mass region.

The authors would like to thank Prof. Yoshi Fujita for his comments concerning the (t,^{3}He) reaction study of ref. [24]. This work has been supported by the EU 6th Framework Programme, "Integrated Infrastructure Initiative - Joint Research Project Activities" Contract number: 506065 (EURONS, JRA11 TRAPSPEC) and by the Academy of Finland under the Finnish Centre of Excellence Programmes 2000-2005 (Project No. 44875, Nuclear and Condenced Matter Physics Programme) and 2006-2011 (Nuclear and Accelerator Based Physics Programme at JYFL).

References

1. G. Lhersonneau *et al.*, Phys. Rev. C **56**, 2445 (1997).
2. W. Urban *et al.*, Nucl. Phys. A **689**, 605 (2001).
3. P. Campbell *et al.*, Phys. Rev. Lett. **89**, 082501 (2002).
4. S. Rinta-Antila *et al.*, Phys. Rev. C **70**, 011301R (2004).
5. U. Hager *et al.*, Phys. Rev. Lett. **96**, 042504 (2006).
6. P. Urkedal, X. Zhang, I. Hamamoto, Phys. Rev. C **64**, 054304 (2001).
7. G. Audi, O. Bersillon, J. Blachot, A. Wapstra, Nucl. Phys. A **729**, 3 (2003).
8. J. Äystö, Nucl. Phys. A **693**, 477 (2001).
9. H. Penttilä *et al.*, Eur. Phys. J. A **25** (s01), 745 (2005).
10. A. Nieminen *et al.*, Nucl. Instrum. Methods Phys. Res. A **469**, 244 (2001).
11. V. Kolhinen *et al.*, Nucl. Instrum. Methods Phys. Res. A **528**, 776 (2004).
12. T. Eronen *et al.*, in preparation.
13. M. König, G. Bollen, H.J. Kluge, T. Otto, J. Szerypo, Int. J. Mass Spectrom. Ion Processes **142**, 95 (1995).
14. A. Jokinen *et al.*, Int. J. Mass Spectrom. **251**, 204 (2006).
15. B. Singh, Nucl. Data Sheets **81**, 1 (1997).
16. I. Band, M. Trzhaskovskaya, J.C.W. Nestor, P. Tikkanen, S. Raman, At. Data Nucl. Data Tables **81**, 1 (2002).
17. D. de Frenne, E. Jacobs, Nucl. Data Sheets **83**, 535 (1998).
18. L. Peker, F. Wohn, J. Hill, R. Petry, Phys. Lett. B **169**, 323 (1986).
19. J. Blachot, Nucl. Data Sheets **64**, 1 (1991).
20. M. Graefenstedt *et al.*, Z. Phys. A **327**, 383 (1987).
21. M. Graefenstedt, U. Keyser, F. Münnich, F. Scheiber, in *Proceedings of the 5th International Conference on Nuclei Far from Stability, Rosseau Lake, Ontario, Canada*, edited by I. Towner (American Institute of Physics, New York, 1988) pp. 30–40.
22. G. Audi, A. Wapstra, C. Thibault, Nucl. Phys. A **729**, 337 (2003).
23. R. Stippler *et al.*, Z. Phys. A **284**, 95 (1978).
24. F. Ajzenberg-Selove, E. Flynn, D. Hanson, S. Orbesen, Phys. Rev. C **19**, 2068 (1979).
25. A. Wapstra, G. Audi, C. Thibault, Nucl. Phys. A **729**, 129 (2003).
26. U. Keyser *et al.*, in *Proceedings of the 6th International Conference on Atomic Masses and Fundamental Constants, East Lansing, MI, USA, Sept. 18-21, 1979*, edited by J.A. Nolen, W. Benenson (Plenum, New York, 1980) pp. 443–449.
27. A. Jokinen *et al.*, Nucl. Phys. A **584**, 489 (1995).
28. J. Wang *et al.*, Eur. Phys. J. A **19**, 83 (2004).
29. J. Skalski, S. Mizutori, W. Nazarewicz, Nucl. Phys. A **617**, 282 (1997).